Estimation of thermal fracture limits in quasi–continuous–wave end–pumped lasers through a time–dependent analytical model

E. H. Bernhardi[1,2], A. Forbes[1,2,*], C. Bollig[1,*] and M. J. D. Esser[1]

[1]*Counsil for Scientific and Industrial Research, National Laser Centre, PO Box 395, Pretoria 0001, South Africa*
[2]*School of Physics, University of KwaZulu–Natal, Private Bag X54001, Durban 4000, South Africa*
[*]*Corresponding authors: aforbes1@csir.co.za and cbollig@csir.co.za*

Abstract: A time–dependent analytical thermal model of the temperature and the corresponding induced thermal stresses on the pump face of quasi–continuous wave (qcw) end-pumped laser rods is derived. We apply the model to qcw diode–end–pumped rods and show the maximum peak pump power that can be utilized without fracturing the rod. To illustrate an application of the model, it is applied to a qcw pumped Tm:YLF rod and found to be in very good agreement with published experimental results. The results indicate new criteria to avoid fracture when operating Tm:YLF rods at low qcw pump duty cycles.

OCIS codes: (140.3480) Lasers, diode–pumped; (140.6810) Thermal effects.

References and links

1. W. Koechner, *Solid-State Laser Engineering* 4th ed., (Springer-Verlag Berlin, Heidelberg, Germany, 1996).
2. C. Pfistner, R. Weber, H. P. Weber, S Merazzi and R. Gruber, "Thermal Beam Distortions in End-Pumped Nd:YAG, Nd:GSGG and Nd:YLF," IEEE J. Quantum Electron. **30**, 1605–1615 (1994).
3. A. K. Cousins, "Temperature and Thermal Stress Scaling in Finite-Length End-Pumped Lasers Rods," IEEE J. Quantum Electron. **28**, 1057–1069 (1992).
4. L. Yan, and C. H. Lee, "Thermal Effects in End-Pumped Nd:phosphate Glasses," J. Appl. Phys. **75**, 1286–1292 (1994).
5. S. Chénais, S. Forget, F. Druon, F. Balembois and P. Georges, "Direct and Absolute Temperature Mapping and Heat Transfer Measurements in Diode-End-Pumped Yb:YAG," Appl. Phys. B **79**, 221–224 (2004).
6. X. Peng, L. Xu and A. Asundi, "High-power efficient continous-wave TEM_{00} intracavity frequency-doubled diode-pumped Nd:YLF laser," Appl. Opt. **44**, 800–807 (2005).
7. G. Barton, *Elements of Green's Functions and Propagation*, (Oxford University Press, Oxford, 1995).
8. H. S. Carslaw and J. C. Jaeger, *Conduction of Heats in Solids*, (Oxford University Press, Oxford, 1959).
9. T. Y. Fan, "Heat Generation in Nd:YAG and Yb:YAG," IEEE J. Quantum Electron. **29**, 1457–1459 (1993).
10. S. P. Timoshenko and J. N. Goodier, *Theory of Elasticity* 3rd ed., (McGraw-Hill, New York, 1970).
11. B. A. Boley and J. H. Weiner, *Theory of Thermal Stresses*, (Courier Dover Publications, New York, 1997).
12. LASCAD Manual, (LASCAD, 2008) , https://www.las-cad.com/files/PP_FEA.pdf.
13. ABAQUS Finite Element Software Package (ABAQUS, 2008) http://www.simulia.com/products/abaqus_fea.html.
14. E. H. Bernhardi, C. Bollig, L. Harris, M. J. D. Esser and A. Forbes, "Investigating thermal stresses in quasi-cw pumped Tm:YLF laser crystals," in *Proceedings of Advanced Solid-State Photonics*, (Nara, Japan, 2008), Poster WB11.
15. S. So, J. I. Mackenzie, D. P. Shepherd, W. A. Clarkson, J. G. Betterson and E. K. Gorton, "A power-scaling strategy for longitudinally diode-pumped Tm:YLF lasers," Appl. Phys. B **84**, 389–393 (2006).
16. M. Pollnau, P. J. Hardman, M. A. Kern, W. A. Clarkson, and D. C. Hanna, "Upconversion-induced heat generation and thermal lensing in Nd:YLF and Nd:YAG," Phys. Rev. B **58**, 16076–16092 (1998).
17. B. M. Walsh, N. P. Barnes, M. Petros, J. Yu, and U. N. Singh, "Spectroscopy and modeling of solid state lanthanide lasers: Application to trivalent Tm^{3+} and $Ho3^{+}$ in $YLiF_4$ and $LuLiF_4$," J. Appl. Phys. **95**, 3255–3271 (2004).

#96267 - $15.00 USD Received 15 May 2008; revised 2 Jul 2008; accepted 9 Jul 2008; published 10 Jul 2008

1. Introduction

The power scaling of diode–end–pumped solid–state lasers is a very active area of research. The main problem that limits the power scaling of these lasers is the generation of heat inside the laser gain medium; the generated heat causes steep temperature gradients inside the crystal, which in turn produce stress, leading to fracture. Fracture of the laser material occurs when the thermally induced stress exceeds the ultimate strength of the material [1]. When the continuous wave (cw) pump power exceeds the power at which crystal fracture occurs, the pump source is often modulated in time, creating a so called quasi–continuous wave (qcw) pump, with the effect of reducing the average pump power to below the fracture limit, while maintaining a high output power during the on-time of the pump pulse.

In order to investigate the thermally induced stresses and the power limitations due to fracture, a thermal model of the laser gain medium is required. Existing analytical thermal models that describe the temperature and stresses in laser crystals are restricted to special cases and approximations, such as cw pump sources and steady–state conditions [1–5]. In this paper an analytical thermal model that determines the transient behaviour of the temperature and the corresponding induced stresses on the pump face of an isotropic laser rod is derived from first principles. To the best of our knowledge this is the first time that such a time–dependent analytical model has been reported. We validate the model through finite element analysis, and apply the model to qcw pumped Tm:YLF laser rods, and find favourable agreement between the calculated fracture limits and the experimentally determined values reported in the literature.

We have particularly chosen to apply the model to a YLF rod because power scaling with this material is limited by the relatively low fracture limit of 40 MPa, which is ~5 times lower than that of YAG [6]. Despite being derived for isotropic rods, we show that the model may be applied to anisotropic rods on condition that the highest linear expansion and the lowest thermal conductivity of the respective a– and c–axis of the crystal are used in the calculation. Finally, we illustrate how the model may be used to estimate the peak pump power that can safely be used to qcw pump a laser rod at a given duty cycle, opening the way to fracture–free power scaling with qcw pump sources.

2. Theory

In this section the transient temperature and stress profiles on the pump face of a longitudinally pumped isotropic laser rod are derived. We assume that the Rayleigh range of the pump beam is much longer than the length of the rod so that the pump beam is treated as perfectly collimated inside the rod. This implies that only the pump face need be considered since the pump light in the gain medium follows an exponential decay, with the steepest temperature gradient (and thus stress) on the pump face [2,4]. A closed form solution for the time dependent temperature profile on the surface of the crystal rod, $u(r,t)$, may be found by solving the non–homogeneous heat diffusion equation [7,8]:

$$\frac{\partial u(r,t)}{\partial t} - D\nabla^2 u(r,t) = Q(r,t), \tag{1}$$

for a generalized source term $Q(r,t)$. Here $D = k/\rho C_p$ is the diffusivity, k is the thermal conductivity, ρ is the density and C_p is the heat capacity of the laser material respectively, while all other terms have their usual meaning. We will assume that the rod has a length l and a radius R, and is homogenous and isotropic. Furthermore, we will assume that the boundary of the rod is at a constant temperature, $u(R,t) = 0$, with no initial temperature profile on its pump face: $u(r,0) = 0$. With these boundary conditions, Eq. (1) may be solved directly by use of an appropriate Green's function, with the solution given in integral form as:

$$u(r,t) = \int_0^t \int_0^R Q(\xi,\tau) G(r,\xi,t-\tau) d\xi d\tau, \tag{2}$$

#96267 - $15.00 USD Received 15 May 2008; revised 2 Jul 2008; accepted 9 Jul 2008; published 10 Jul 2008

with the Green's function $G(r,\xi,t)$ given by [7]:

$$G(r,\xi,t)=\sum_{m=1}^{\infty}\frac{2\xi}{R^2J_1^2(\mu_m)}J_0(\mu_m r/R)J_0(\mu_m r/R)\exp\left(-\frac{D\mu_m^2 t}{R^2}\right). \quad (3)$$

The summation is over the positive roots (μ_m) of the zeroth order Bessel function, J_0. For the common experimental configuration where the pump beam is imaged onto the rod face from a multimode fibre, the pump intensity may be approximated as having a top–hat spatial intensity profile. Figure 1 shows an example of a measured top–hat transverse intensity profile as produced by a fibre–coupled diode pump. If in addition the pump is not assumed to be cw but rather the more general qcw, consisting of a pulse train of on–off pulses with on–time τ_{on} (with τ_{on} usually longer than the upper–state lifetime of the laser gain medium) and period T, we may write the source term as:

$$Q(r,t)=\begin{cases}\dfrac{\alpha\eta E}{\pi w^2\rho C_p\tau_{on}} & ;nT\le t\le nT+\tau_{on}\\ 0 & ;nT+\tau_{on}\le t\le (n+1)T\end{cases}, \quad (4)$$

where n is the number of pulses, E is the energy in each pulse and w is the radius of the top–hat beam. α is the absorption coefficient in units of inverse length of the crystal, while η is a parameter to account for the fact that not all the absorbed pump light is converted into heat. This model can be applied under lasing or non–lasing conditions by choosing an appropriate value for η. Typical values for the heat load efficiency are η=0.32 (lasing) and η=0.4 (non–lasing) [9].

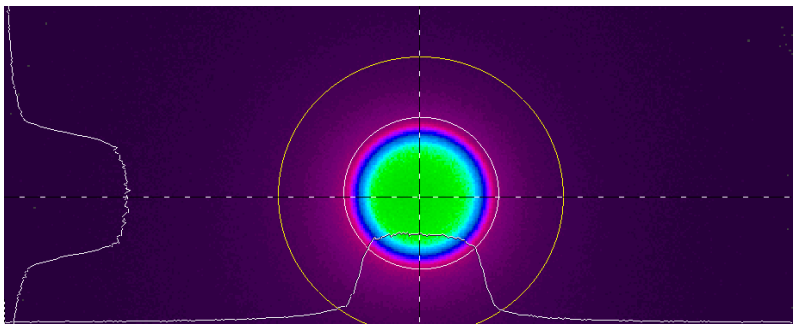

Fig. 1. An example of a measured top–hat transverse intensity profile produced by a fibre coupled diode laser pump (own experimental results).

Substituting Eqs. (3) and (4) into Eq. (2) and solving both the time and spatial integrals separately yields the following analytical expression for the temperature on the pump face of the rod:

$$u(r,pT+t)=\frac{2\alpha\eta ER}{k\pi w\tau_{on}}\sum_{m=1}^{\infty}\frac{J_0(\mu_m r/R)J_1(\mu_m w/R)f(p,t,\mu_m)}{\mu_m^3J_1^2(\mu_m)}, \quad (5)$$

with the time dependence given by $f(p,t,\mu_m)$ as:

#96267 - $15.00 USD Received 15 May 2008; revised 2 Jul 2008; accepted 9 Jul 2008; published 10 Jul 2008

$$f(p,t,\mu_m)=\exp\left(-\mu_m^2\frac{t}{\tau_D}\right)\left\{\frac{\left[\exp\left(\mu_m^2\frac{\tau_{on}}{\tau_D}\right)-1\right]\left[\exp\left(-\mu_m^2\frac{pT}{\tau_D}\right)-1\right]}{1-\exp\left(\mu_m^2\frac{T}{\tau_D}\right)}-\left[1-\exp\left(\mu_m^2\frac{\tau}{\tau_D}\right)\right]\right\}, \quad (6)$$

with $\tau = \min[t, \tau_{on}]$. Here we have introduced a new variable, $\tau_D = R^2/D$, which we refer to as the diffusion relaxation time of the system, and for convenience the temperature is calculated after p complete pulses plus some time t into the p+1 pulse, so that the total elapsed time from the start of the pumping process is $pT + t$. While the summation in Eq. (5) is carried to infinity, in practice one finds that 30 terms or above leads to very good convergence of the series. Equation (5) may easily be rewritten in terms of peak pump power (P_p) or average pump power (P_{av}) rather than pump energy (E) by noting that for the source term in this study $P_p = E/\tau_{on}$ and $P_{av} = E/T$ (note: here we have assumed that the time pulse envelope is a square pulse; for other cases the peak pump power expression may have to be modified in an appropriate manner). In the special case of a cw pump source, $T = \tau_{on}$ so that the peak and average pump powers are identical.

By making use of a plane–strain approximation and assuming that the stress in the axial direction is zero, we may calculate the radial and tangential stresses from the temperature profile from [10,11]:

$$\sigma_r(r,t)=C\left[\frac{1}{R^2}\int_0^R u(r,t)rdr-\frac{1}{r^2}\int_0^r u(r,t)rdr\right]; \quad (7a)$$

$$\sigma_\theta(r,t)=C\left[\frac{1}{R^2}\int_0^R u(r,t)rdr+\frac{1}{r^2}\int_0^r u(r,t)rdr-u(r,t)\right], \quad (7b)$$

where $C = \gamma Y/(1-\upsilon)$, with γ the linear coefficient of expansion, Y is Young's modulus and υ is Poisson's ratio. The plain–strain approximation is valid for $l/R >> 1$ (a long rod) [11]. For the case where $l/R << 1$ (a thin disk), the plane–stress approximation is used where Eqs. (7a) and (7b) also hold with $C = \gamma Y$ [11]. One can readily show that Eqs. (7a) and (7b) can be solved analytically to yield:

$$\sigma_r(r,pT+t)=\frac{2C\alpha\eta ER}{k\pi w\tau_{on}}\sum_{m=1}^{\infty}\frac{J_1(\mu_m w/R)}{\mu_m^3 J_1^2(\mu_m)}\left[\frac{J_1(\mu_m)}{\mu_m}-\frac{RJ_1(\mu_m r/R)}{r\mu_m}\right]f(p,t,\mu_m); \quad (8a)$$

$$\sigma_\theta(r,pT+t)=\frac{2C\alpha\eta ER}{k\pi w\tau_{on}}\sum_{m=1}^{\infty}\frac{J_1(\mu_m w/R)}{\mu_m^3 J_1^2(\mu_m)}\left[\frac{J_1(\mu_m)}{\mu_m}+\frac{RJ_1(\mu_m r/R)}{r\mu_m}-J_0(\mu_m r/R)\right]f(p,t,\mu_m). \quad (8b)$$

Due to the fact that the stress tensor alone does not provide enough information regarding crystal fracture, we use the maximum shear stress to predict fracture [12]. This is also known as the stress intensity or the Tresca failure criterion, which in the plain–strain approximation reduces to:

$$\begin{aligned}\sigma_T(r,pT+t)&=\left|\sigma_\theta-\sigma_r\right|\\&=\left|\frac{2C\alpha\eta ER}{k\pi w\tau_{on}}\sum_{m=1}^{\infty}\frac{J_1(\mu_m w/R)}{\mu_m^3 J_1^2(\mu_m)}J_2(\mu_m r/R)f(p,t,\mu_m)\right|,\end{aligned} \quad (9)$$

#96267 - $15.00 USD Received 15 May 2008; revised 2 Jul 2008; accepted 9 Jul 2008; published 10 Jul 2008

where we have made use of the well known relation $J_2(x) = 2J_1(x)/x - J_0(x)$. Equations (5), (8) and (9) allow the temperature, stresses and fracture limit to be calculated for any qcw pulse train, as a function of both time and position in the crystal rod.

3. Model validation

As a verification of the analytical thermal model, a time–dependent three dimensional coupled thermal–stress finite element analysis was implemented in a commercial software package, ABAQUS [13,14]. The average computation time of each finite element simulation (5560 discretization) was approximately 5.5 hours on a dual–core 2.4 GHz processor (the analytical model takes ~1–2 s). In analogy with convective heat transfer, we have specified a Neumann boundary condition with a heat transfer coefficient at the interface between the crystal and the copper heat sink. We have used a heat transfer coefficient of 0.9 $Wcm^{-2}K^{-1}$, which corresponds to a layer of indium foil between the crystal and the heat sink [5]. In the remaining text the finite element analysis will be referred to as the *numerical* model [14].

The analytical and numerical models have been applied to reported results [15] of a cw pumped, 4% doped, Tm:YLF laser rod with l = 12 mm and R = 1.5 mm (l/R=8 so that we make use the plain–strain approximation as discussed in section (2)). The pump beam was a near top–hat profile with M^2 ~100 and a pump radius of w = 470 μm in the middle of the crystal. The onset of fracture was reported at an incident power of 47.2 W (α = 1.43 cm^{-1}; η = 0.33). While the actual stress values at fracture are not reported, it is known that the fracture limit of YLF crystals is in the 33–40 MPa range [1,6]. The parameters that were used in the numerical and analytical thermal models are shown in Table 1.

The analytical model predicts a maximum Tresca stress of 42 MPa which agrees very well with the reported 33–40 MPa fracture limit range [1,6]. The numerical model results in a maximum Tresca stress of 41 MPa. This shows that for a cw pump, the analytical thermal model is consistent with both the experimental fracture data and with the numerical solutions of a three–dimensional finite element analysis. Since the analytical thermal model proved to be accurate for a cw pump beam, the transient behaviour of the temperature and the induced stresses were determined for various qcw pump duty cycles, defined as τ_{on}/T. Figure 2(a) and 2(b) show the predicted time–dependence of the temperature in the centre of the pump face of the Tm:YLF rod for a 10% and a 50% pump duty cycle respectively (τ_{on} = 10 ms). The upper and lower boundaries of the shaded red region in Fig. 2 indicate the analytical model's predictions of the temperature when the thermal conductivity of the c– and the a–axis of Tm:YLF were used respectively. It is clear from the graphs that there is very good agreement between the analytical and numerical models when the lowest thermal conductivity is used in the calculations. Figure 3 illustrates that the thermally induced stresses as calculated by the two models show very good agreement when the highest linear expansion coefficient is used in the analytical model. The upper and lower boundaries of the shaded red region in Fig. 3 indicate the analytical model's predictions of the maximum stress on the pump face when the two respective linear expansion coefficients of Tm:YLF were used along with the lowest thermal conductivity.

By considering the transient stress distribution on the entire pump face with a qcw pump source, it is evident that the maximum stress does not always occur on the edge–surface ($r = R$) of the rod; this is contrary to the case of a cw pump beam [4]. The position of the maximum stress changes during a single qcw pump pulse as well as between qcw pulses. Figure 4(a) shows an animation of the analytically predicted σ_T on the pump face of the Tm:YLF rod when subjected to a 90 W peak power pump beam at 50 Hz (T = 20 ms; τ_{on} = 10 ms), while Fig. 4(b) shows an animation of the numerically predicted σ_T throughout the bulk of the Tm:YLF rod. A cross–section of the stress is overlaid on the analytical animation, and clearly shows the "peak" where the stress is maximum and its movement in time as the pulses accumulate. Note that the numerical solution does not exhibit the same symmetrical stress distribution on the pump face as the analytical solution since the anisotropic characteristics of Tm:YLF were accounted for in the numerical model and not in the analytical model.

#96267 - $15.00 USD Received 15 May 2008; revised 2 Jul 2008; accepted 9 Jul 2008; published 10 Jul 2008

Table 1. Parameter values of the pumped Tm:YLF rod that were implemented in the simulations.

Parameter	*Thermal Model*	*Reference*
Pump beam radius (w) [mm]	0.47	[15]
Rod radius (R) [mm]	1.5	[15]
Absorption coefficient (α) [cm^{-1}]	1.43	[15]
Thermal conductivity (k) [$W.m^{-1}.K^{-1}$]	7.2 (a-axis), 5.8 (c-axis)	[1,16]
Linear expansion coefficient (γ) [10^{-6} K^{-1}]	13 (a-axis), 8.0 (c-axis)	[1,17]
Fractional heat load (η)	0.33	estimated
Poisson's ratio (υ)	0.33	[1,16]
Young's modulus (Y) [GPa]	75	[1,2]
Density (ρ) [$g.cm^{-3}$]	3.9	[1,17]
Specific heat capacity (C_p) [$J.g^{-1}.K^{-1}$]	0.79	[1,17]

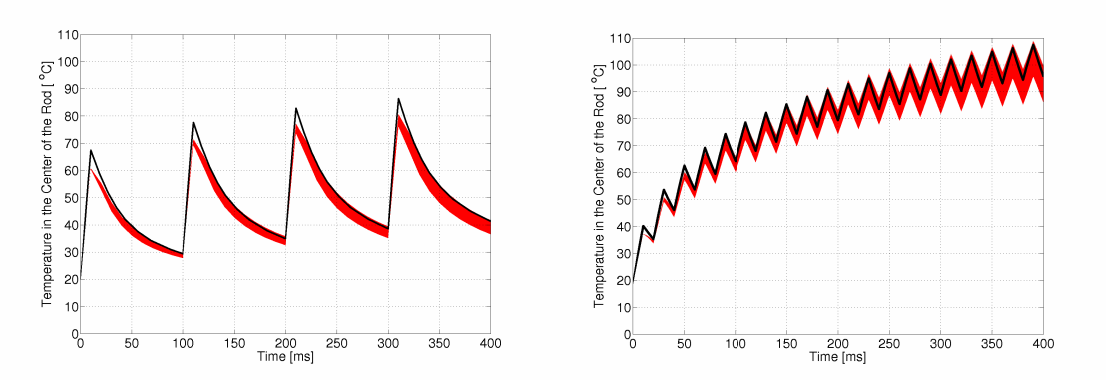

(a) (b)

Fig. 2. The analytically (red) and numerically (black) predicted temperature in the centre of the Tm:YLF rod as a function of time while the rod is subjected to a qcw pump with a peak power of (a) 200 W at 10 Hz (τ_{on} = 10 ms) and, (b) 90 W at 50 Hz (τ_{on} = 10 ms).

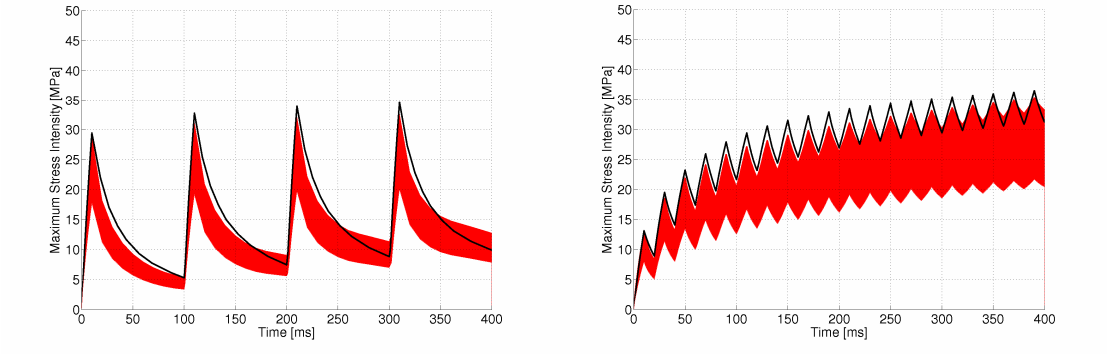

(a) (b)

Fig. 3. The maximum stress on the pump face of the Tm:YLF rod as a function of time while the rod is subjected to a qcw pump with a peak power of (a) 200 W at 10 Hz (τ_{on} = 10 ms), and (b) 90 W at 50 Hz (τ_{on} = 10 ms). The analytical (red) and numerical (black) solutions are shown.

#96267 - $15.00 USD Received 15 May 2008; revised 2 Jul 2008; accepted 9 Jul 2008; published 10 Jul 2008

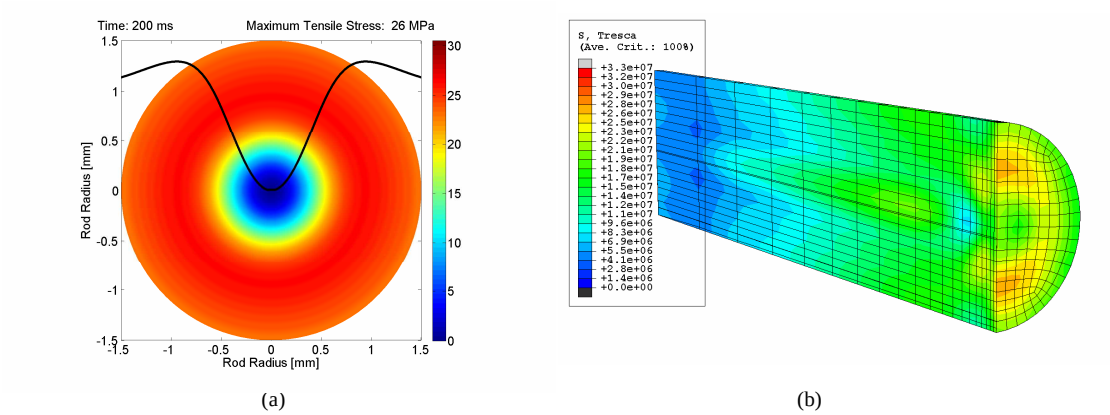

(a) (b)

Fig. 4. (0.75 MB and 0.33 MB respectively) Animations of (a) the analytical stress distribution on the pump face and (b) the numerical stress distribution in volume of the Tm:YLF rod while it is subjected to a 90 W peak power qcw pump beam at 50 Hz (τ_{on} = 10 ms).

4. Power scaling of Tm:YLF rods by qcw pumping

To achieve ever higher output powers from a diode–end–pumped solid state laser, the pump power itself must be increased in a concomitant manner. When the pump is a cw source, the high average powers required in some applications leads to high thermal loads, and the onset of fracture. A standard solution to this problem is to employ a qcw pump source, with the advantages that: (i) the average thermal load is reduced through a reduced duty cycle, and (ii) the qcw pulsing leads to higher peak pump power, resulting in much higher laser output power during the qcw pump pulses.

During the qcw operation of a solid–state laser, the generally accepted criteria to avoid thermal fracture is to pump the crystal with an average power (P_{av}) that is below the cw fracture pump power (P_{cw}):

$$P_{av} \leq P_{cw}. \tag{10}$$

The thermal model developed in section (2) provides a more comprehensive criterion for safe qcw operation, through direct application of Eq. (9), and the results are shown in Fig. 5. The green shaded area in Fig. 5(a) shows the analytically predicted average power with which the Tm:YLF crystal can be pumped without causing thermal fracture, while the red region indicate the predicted onset of fracture using Eq. (10). The yellow region then indicates the region of disagreement between the two models. It is clear that for qcw pump duty cycles of 40% and higher, fracture of the Tm:YLF rod will indeed occur at average pump powers which are equal or greater to the cw fracture pump power, so that Eqs. (9) and (10) are in agreement. At pump duty cycles that are lower than 40%, the analytical model predicts that crystal fracture will occur at average powers that are significantly lower than the cw fracture pump power. By way of example, consider a qcw pump duty cycle of 10% (T = 100 ms; τ_{on} = 10 ms) where the fracture limit of Tm:YLF is at P_{cw} = 47 W. For this qcw duty cycle, fracture would occur at P_{av} > 26 W, with the region 47 W >P_{av} > 26 W indicating the error of using Eq. (10). This error is indicated for all duty cycles as the yellow shaded area in Fig. 5(a). The implication is that Eq. (10) is a necessary but not sufficient condition for fracture–free qcw operation in Tm:YLF lasers.

An alternative approach to illustrate the results of the analytical thermal model is to consider the peak power during a qcw pump pulse and to note the peak power at which fracture occurs. The green shaded area in Fig. 5(b) indicates the qcw peak power that can be used to pump the Tm:YLF rod without fracturing it as predicted by the analytical model, while the red region indicates the fracture limit using Eq. (10); the yellow region is once again the region of discrepancy.

#96267 - $15.00 USD Received 15 May 2008; revised 2 Jul 2008; accepted 9 Jul 2008; published 10 Jul 2008

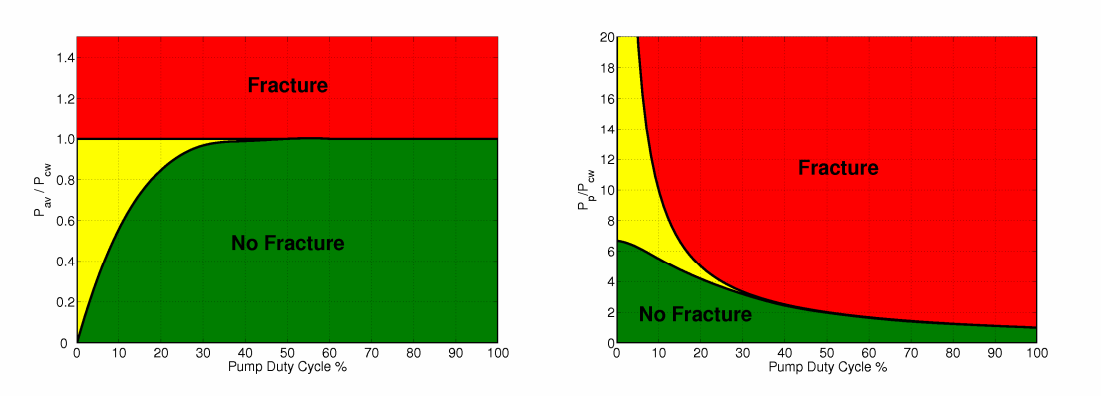

(a) (b)

Fig. 5. (a). The average pump power (as a fraction of the cw fracture power P_{cw}) at which fracture of the Tm:YLF rod occurs as a function of qcw pump duty cycle (τ_{on} = 10 ms). The green shaded region indicates the average pump power at which the Tm:YLF rod can be pumped without fracturing according to the analytical model. The yellow shaded region indicates the difference between the analytical model and $P_{cw.}$ (b) The same notation as in (a) but for the peak pump power (in units of P_{cw}) at which fracture of the Tm:YLF rod occurs as a function of qcw pump duty cycle.

Considering the qcw pump duty cycle of 10%, we note that the Tm:YLF rod can be pumped with a peak pump power of 5.5× higher (270 W) than the cw fracture power before fracture will occur, while Eq. (10) would predict a 10× higher value (470 W).

The model predictions can thus be summarised as follows: the rule of thumb given by Eq. (10) is a necessary but not sufficient condition for fracture–free power scaling of Tm:YLF through the use of qcw pump sources. This is not surprising given that this criteria is not derived from an analysis of the onset of fracture, but is based rather on intuition. Equation (9) is derived from a full thermal analysis, and we suggest that this provides the necessary criterion for any laser rod to be pumped without fracture. In the limit that the duty cycle approaches the cw case, Eq. (9) correctly converges to Eq. (10) as expected.

5. Conclusion

A time–dependent analytical thermal model was developed to investigate the transient behaviour of thermally induced stresses in qcw end–pumped laser rods. The versatility of such a model is that all the material and pump laser parameters may be varied analytically, thereby aiding physical insight. For example, the model confirms exactly that the temperature increases linearly with pump power, as expected. Similarly, one can 'instantaneously' determine how the rod temperature varies with any of the key parameters, enabling one to easily probe the underlying physics with questions such as: how does the temperature profile vary with pump size *w*? Determining this numerically would be extremely time consuming. Furthermore, the resulting analytical expression for the temperature of the rod may be used to determine other quantities, such as the optical aberrations likely to be imparted to a propagating wave through the crystal rod. The key advantages of the analytical model are ease of computation, as highlighted above, and time of computation. We reported that the average computation time of each finite element simulation was approximately 5.5 hours on a dual–core 2.4 GHz processor; this is in stark contrast to the analytical model in which the computational time is less than a couple of seconds on a standard PC, i.e., for all practical purposes it is 'instantaneous' in comparison.

The analytical model was used to investigate the thermal stress in a Tm:YLF rod at various qcw pump duty cycles, and was found to be in very good agreement with that of a time–dependent coupled thermal–stress finite element analysis, and with published experimental data. We have applied the analytical model to determine the maximum peak

#96267 - $15.00 USD Received 15 May 2008; revised 2 Jul 2008; accepted 9 Jul 2008; published 10 Jul 2008

power at which a Tm:YLF rod can be pumped before it will fracture. We show that at all qcw duty cycles the crystal will fracture at average power levels that are lower than predicted by using the corresponding cw fracture limit. The discrepancy is largest at low duty cycles, converging to a perfect agreement in the limiting case of a 100% duty cycle (cw). Thus we suggest a new criteria to be applied for safe power scaling of Tm:YLF rods. While the implementation of the analytical model has concentrated on YLF due to its low fracture limit, the model presented here may be applied to any end–pumped laser rod pumped using qcw or cw sources as the assumptions used to develop the analytical model are not material specific. It needs to be verified for other gain materials and other pumping conditions that the same discrepancy (between the predicted average power level at which fracture will occur and the cw fracture limit) exists at low duty cycles.

#96267 - $15.00 USD Received 15 May 2008; revised 2 Jul 2008; accepted 9 Jul 2008; published 10 Jul 2008